

# Model polymer nanocomposites provide an understanding of confinement effects in real nanocomposites

PERLA RITTIGSTEIN<sup>1</sup>, RODNEY D. PRIESTLEY<sup>1</sup>, LINDA J. BROADBELT<sup>1</sup> AND JOHN M. TORKELSON<sup>1,2\*</sup>

<sup>1</sup>Department of Chemical and Biological Engineering, Northwestern University, Evanston, Illinois 60208-3120, USA

<sup>2</sup>Department of Materials Science and Engineering, Northwestern University, Evanston, Illinois 60208-3120, USA

\*e-mail: j-torkelson@northwestern.edu

Published online: 18 March 2007; doi:10.1038/nmat1870

Owing to the improvement of properties including conductivity, toughness and permeability, polymer nanocomposites are slated for applications ranging from membranes to fuel cells<sup>1,2</sup>. The enhancement of polymer properties by the addition of inorganic nanoparticles is a complex function of interfacial interactions, interfacial area and the distribution of inter-nanofiller distances. The latter two factors depend on nanofiller dispersion, making it difficult to develop a fundamental understanding of their effects on nanocomposite properties. Here, we design model poly(methyl methacrylate)–silica and poly(2-vinyl pyridine)–silica nanocomposites consisting of polymer films confined between silica slides. We compare the dependence of the glass-transition temperature ( $T_g$ ) and physical ageing on the interlayer distance in model nanocomposites with the dependence of silica nanoparticle content in real nanocomposites. We show that model nanocomposites provide a simple way to gain insight into the effect of interparticle spacing on  $T_g$  and to predict the approximate ageing response of real nanocomposites.

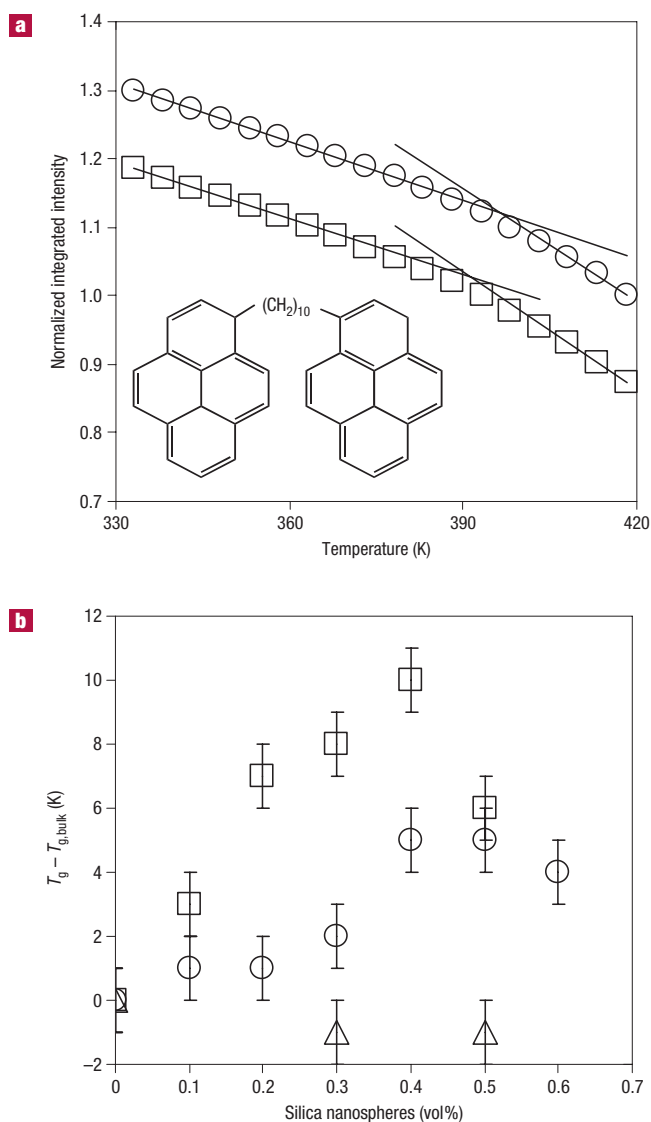
The effect of nanoscale confinement on  $T_g$  has been studied in polymers since the mid 1990s<sup>3–15</sup>. With ultrathin films, deviations from bulk  $T_g$  ( $T_{g,bulk}$ ) as large as 45–50 K in supported films<sup>4,11</sup> and 70 K in free-standing films<sup>5</sup> have been reported. In supported films, the thickness dependence of  $T_g$  is affected by polymer–substrate interactions<sup>3,4,6–8,12</sup> and the free surface<sup>3,5,10,11,13</sup>, the impact of which increases as the ratio of interfacial area to volume increases. At the free surface,  $T_g$  is reduced compared with  $T_{g,bulk}$ , as revealed by fluorescence measurements<sup>10</sup>. This effect propagates into the film<sup>10</sup>, reducing the  $T_g$  of ultrathin free-standing films and supported films lacking attractive polymer–substrate interactions. Thus, the  $T_g$  reduction originates with the free-surface effect; as shown recently<sup>10</sup>, nanoconfinement itself only affects the magnitude of the  $T_g$  gradient within the film. With moderate-to-strong attractive polymer–substrate interactions, for example, hydrogen bonds between oxygen atoms in poly(methyl methacrylate) (PMMA) or nitrogen atoms in poly(2-vinyl pyridine) (P2VP) and hydroxyl groups on silica surfaces,  $T_g$  increases with decreasing thickness<sup>4,6–9,12</sup>. In nanocomposites with well-dispersed nanofiller,  $T_g$  can exhibit substantial deviations relative to the bulk polymer<sup>16–21</sup>, decreasing when polymer–nanofiller interfaces yield free surfaces<sup>16,21</sup> and increasing when wetted interfaces with attractive interactions result<sup>21</sup>. These outcomes in nanocomposites were predicted through simulation<sup>22</sup> before their experimental demonstration<sup>16,21</sup>.

In contrast to the many studies of the  $T_g$ -confinement effect<sup>3–15</sup>, fewer studies have addressed the effect of confinement on physical ageing of neat polymers<sup>9,23–26</sup> or polymer nanocomposites at low nanoparticle loadings<sup>21,27</sup>. (Physical ageing is the change in properties as a function of annealing time below  $T_g$  that accompanies the spontaneous relaxation of a non-equilibrium glass towards equilibrium.) In films or nanocomposites without attractive interfacial interactions, for example, polystyrene (PS)–silica systems, there is in general no significant effect of confinement on ageing at a constant quench depth below  $T_g$  (ref. 23). An exception occurs at temperatures near but below  $T_{g,bulk}$ , where bulk polymer ages but ultrathin films with reduced  $T_g$  values are at equilibrium<sup>23,26</sup>. In contrast, ageing is suppressed in confined films or nanocomposites with attractive interfacial interactions<sup>21,23,24,27</sup>.

Here, we compare the  $T_g$  values of ‘model’ and ‘real’ polymer–silica nanocomposites. Model nanocomposites are made from doubly supported films lacking a free surface. This structure is achieved by spin-coating two films supported on silica slides, laying one atop the other, and annealing to heal the interface. This yields a consolidated film with a constant interlayer distance between silica surfaces. Model nanocomposites allow for quantitative determination of the effect of silica interlayer distance on the polymer  $T_g$ . We find that model and real nanocomposites with identical  $T_g$  deviations yield similar dramatic suppressions of physical ageing. This indicates that model nanocomposites can be broadly useful in studying amorphous polymer nanocomposites with wetted interfaces.

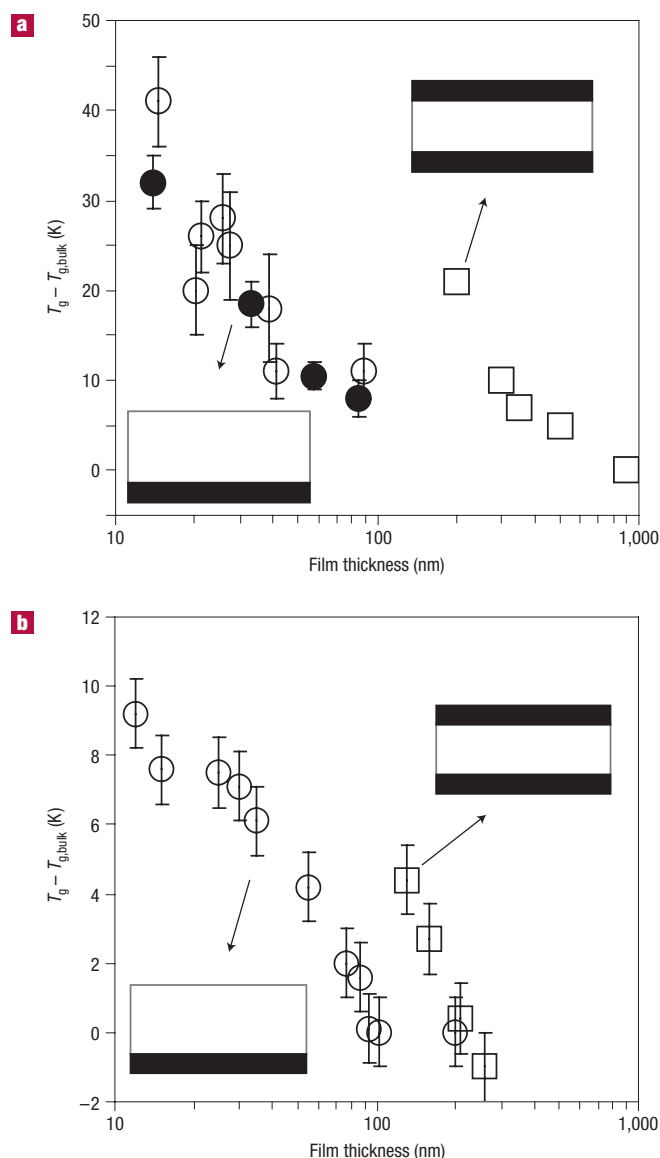
Fluorescence has been used to characterize  $T_g$  and ageing in confined polymers<sup>9–12,21,23,24</sup> and is used here to characterize these properties in model and real nanocomposites. Figure 1a shows the temperature dependence of the fluorescence of 1,10-bis(1-pyrene)decane (BPD) doped at trace levels into bulk PMMA and a 0.4 vol% silica–PMMA nanocomposite. The  $T_g$  is identified by the intersection of linear fits in the liquid and glassy states. The  $T_g$  of the nanocomposite is increased by 5 K relative to that of bulk PMMA.

Figure 1b summarizes the effect of nanoparticle loading on the  $T_g$  values of P2VP-, PMMA- and PS-silica nanocomposites. Within experimental uncertainty, adding 0.5 vol% silica (10- to 15-nm-diameter nanoparticles) has no effect on the  $T_g$  of PS. This is in accord with a study<sup>10</sup> of bulk PS bilayer films showing that a 14-nm-thick layer at the silica substrate interface exhibits  $T_{g,bulk}$ .



**Figure 1**  $T_g$  data from bulk polymer and polymer nanocomposites determined via fluorescence. **a**, Temperature dependence of the normalized fluorescence integrated intensity of BPD dopant (<0.2 wt%) in a bulk PMMA film (open squares) and in a 0.4 vol% silica–PMMA nanocomposite film (open circles). Inset: The molecular structure of BPD. (The data have been normalized to 1 relative to the intensity at  $T_{g,bulk}$  and arbitrarily shifted vertically.) **b**, Deviations from  $T_{g,bulk}$  as a function of silica nanofiller content in three polymer nanocomposites: P2VP (open squares), PMMA (open circles) and PS (open triangles). The error bars ( $\pm 1$  K) represent the inherent error due to the fitting of the data required to obtain  $T_g$ .

We note that a recent study<sup>28</sup> reported a decrease in  $T_g$  of  $\sim 11$  K when 40 wt% ( $\sim 18$  vol%) silica nanoparticles identical to those used here were added to PS; this  $T_g$  reduction was ascribed to the presence of free surfaces at the non-wetted interfaces of the PS and silica nanoparticles that were not well dispersed. When nanoparticle loading was reduced to 2 wt% ( $\sim 0.9$  vol%), near the concentrations used here, there was no change in  $T_g$  from that of bulk PS, consistent with our results. In contrast, the P2VP– and PMMA–silica nanocomposites exhibit enhancements in  $T_g$  at silica loadings as low as 0.1–0.3 vol%. The apparent maximum 5 and 10 K enhancements in the  $T_g$  values obtained with 0.4–0.5 vol% silica in the PMMA and P2VP nanocomposites, respectively, are



**Figure 2** Deviations of  $T_g$  from  $T_{g,bulk}$  of ultrathin films supported on silica and ‘model’ nanocomposites. **a**, Thickness dependence of the  $T_g$  deviation of P2VP supported films (open circles: data from ref. 4; filled circles: data from ref. 8) and pyrene-doped P2VP ‘model’ nanocomposites (open squares). (In the case of the P2VP supported films, the error bars are from refs 4,8 and in the case of the P2VP ‘model’ nanocomposites, the error ( $\pm 1$  K) in the data is due to the fitting required to obtain  $T_g$  and is smaller than the symbol size.) **b**, Thickness dependence of the  $T_g$  deviation of TC1-labelled PMMA supported films (open circles) and ‘model’ nanocomposites (open squares). The error bars ( $\pm 1$  K) represent the inherent error due to the fitting of the data required to obtain  $T_g$ .

hypothesized to result from decreases in nanoparticle dispersion achieved at higher loadings.

It is well known that PMMA and P2VP experience hydrogen-bonding interactions with silica surfaces containing hydroxyl groups<sup>4,7,9,24</sup>, whereas PS does not. The enhanced  $T_g$  values observed in the PMMA–silica nanocomposites in Fig. 1b arise from these attractive polymer–nanoparticle interfacial interactions that reduce cooperative segmental mobility. Similar effects are expected in P2VP–silica nanocomposites. (We note that recent studies<sup>29,30</sup>

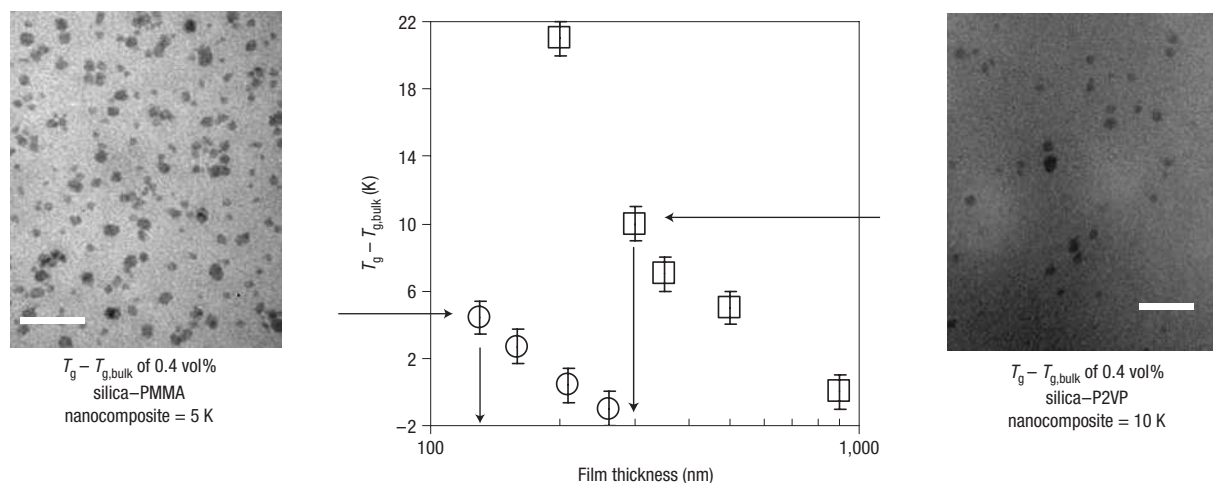


**Figure 3** Interlayer spacing (film thicknesses) in 'model' nanocomposites that yield the same  $T_g$  deviation as 0.4 vol% silica-PMMA and silica-P2VP nanocomposites.  $T_g$  deviations of P2VP 'model' nanocomposites (open squares) and PMMA 'model' nanocomposites (open circles). Right and left: Transmission electron microscopy images of 0.4 vol% silica-P2VP (right) and 0.4 vol% silica-PMMA (left) nanocomposites (scale bars = 100 nm). The error bars ( $\pm 1$  K) represent the inherent error due to the fitting of the data required to obtain  $T_g$ .

indicate that nanoparticle-polymer interactions lead to internal stresses within polymer nanocomposites. We do not discount the possibility that such stresses may affect relaxation dynamics in nanocomposites, including those associated with  $T_g$ .)

There are two complications in developing a fundamental understanding of the effects of nanoparticle loading and interparticle distance on  $T_g$  in well-dispersed nanocomposites. First, there is a wide distribution of interparticle distances, and, second, the  $T_g$  dynamics of polymer segments may be impacted by any number of nanoparticles located within a radius of tens to even hundreds of nanometres. To eliminate these complications, we developed model nanocomposites with a known constant interlayer spacing by confining polymer films between silica slides. Figure 2 shows  $T_g - T_{g,bulk}$  as a function of thickness for both ultrathin films supported on silica and model nanocomposites of P2VP and PMMA. As illustrated in Fig. 2, replacement of the free surface in the films by a silica interface (model nanocomposites) with attractive interfacial interactions leads to an increase in the length scale at which  $T_g$ -confinement effects are observed. For example, a 21 K enhancement of  $T_g$  is observed in both a 200-nm-thick P2VP-silica model nanocomposite and a 30-nm-thick P2VP film supported on silica (one free surface). Similarly, a 4–5 K enhancement of  $T_g$  is observed in both a 130-nm-thick PMMA-silica model nanocomposite and a 55-nm-thick PMMA film supported on silica (one free surface).

Remarkably, the length scale at which confinement effects are observed in model nanocomposites can be hundreds of nanometres. In particular, P2VP model nanocomposites show a 5 K enhancement of  $T_g$  relative to bulk at a thickness (interlayer spacing) of 500 nm. This is the largest length scale for which an effect of confinement on  $T_g$  has been reported and indicates that these effects can be microscale when strong attractive interactions are present.

Figure 3 shows micrographs of 0.4 vol% silica nanocomposites indicating good nanoparticle dispersion. From the  $T_g$  comparison between real and model nanocomposites presented in Fig. 3, the  $T_g$  enhancement in the real P2VP nanocomposite is equal to that of a model nanocomposite with an approximately 300 nm interlayer spacing, whereas the  $T_g$  enhancement in the real PMMA nanocomposite is equal to that of a model nanocomposite with

an approximately 130 nm interlayer spacing. Consistent with the fact that the nanoparticles have diverse interparticle spacings, the 130 and 300 nm 'effective average' interlayer spacings are greater than the  $\sim 50$  nm theoretical interparticle distance (silica surface to silica surface) determined assuming an ideal cubic dispersion of nanoparticles. These 'effective average' interlayer spacings determined by comparison with model nanocomposites provide a simple approach for quantifying the extent to which confinement effects involving attractive interactions at nanofiller interfaces modify polymer  $T_g$  behaviour.

Likewise, model nanocomposites can also be useful in roughly predicting the physical ageing behaviour of real nanocomposites. Figure 4 shows the results of fluorescence studies characterizing ageing in bulk P2VP and real and model nanocomposites, the latter two exhibiting the same 10 K confinement-induced  $T_g$  enhancement. During ageing, an increase in fluorescence intensity correlates with a several orders-of-magnitude smaller increase in density<sup>21,23,24</sup>. The roughly linear increase in intensity with logarithmic ageing time in bulk P2VP is consistent with the manner in which physical ageing leads to changes in properties, including density. When aged at 303 K, bulk P2VP exhibits a 35% increase in fluorescence intensity over 8 h. However, both model and real P2VP-silica nanocomposites exhibit dramatically suppressed physical ageing, meaning that model nanocomposites can serve as an appropriate system for studying a range of glassy-state behaviour in real nanocomposites.

These results are consistent with a study showing a near elimination of ageing in interfacial layers of a bulk PMMA film supported on silica<sup>24</sup>. These results also indicate that interfacial interactions that yield significant increases in  $T_g$  in nanocomposites may yield much more significant effects on other glassy behaviour such as physical ageing. This suggests that nanocomposites may lead to the production of glassy-state polymeric systems with properties that are nearly stable during long-term use.

The technological importance and significant scientific questions associated with the very long-range, confinement-related enhancements in  $T_g$  and the suppression of physical ageing observed in polymers undergoing attractive interfacial interactions provide further impetus to study confinement effects in polymer nanocomposites. Model nanocomposites with silica and other

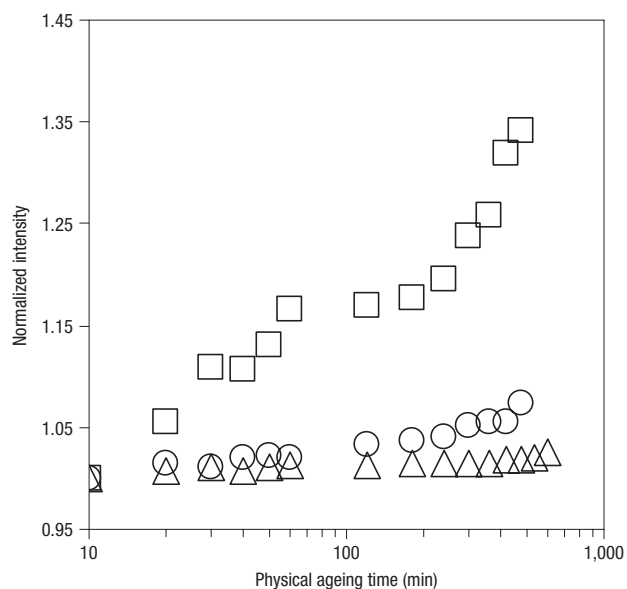


**Figure 4** Physical ageing of bulk polymer and polymer nanocomposites monitored by fluorescence. Normalized fluorescence intensity of TCJ dopant (<0.2 wt%) as a function of logarithmic physical ageing time after a quench from above  $T_g$  (413 K) to below  $T_g$  (303 K): bulk P2VP film (open squares), 0.4 vol% silica-P2VP nanocomposite (open circles), and 300-nm-thick P2VP 'model' nanocomposite (open triangles). The physical ageing rates are related to the slopes of the data sets.

substrates yield well-designed systems for such investigations. Further studies are underway.

## METHODS

### MATERIALS SYNTHESIS AND CHARACTERIZATION

PS (Pressure Chemical,  $M_n = 290,000 \text{ g mol}^{-1}$ ,  $M_w/M_n = 1.06$ ) was used as received. PMMA was synthesized by free-radical polymerization ( $M_n = 355,000 \text{ g mol}^{-1}$ ,  $M_w/M_n = 1.54$ , by gel permeation chromatography using universal calibration with PS standards). 4-tricyanovinyl-[N-(2-hydroxyethyl)-N-ethyl]aniline (TC1)-labelled PMMA ( $M_n = 509,000 \text{ g mol}^{-1}$ ,  $M_w/M_n = 1.67$  by gel permeation chromatography using universal calibration with PS standards) was synthesized by reacting methyl methacrylate monomer in the presence of a trace amount of TC1-labelled methacrylate monomer. The TC1-labelled monomer was synthesized following ref. 24. TC1-labelled PMMA contained 1.37 mol% labelled monomer, as determined by ultraviolet absorbance. After synthesis, PMMA and TC1-labelled PMMA were washed by multiple dissolving/precipitating steps in toluene/methanol and dried *in vacuo* at 410 K for 24 h. P2VP (Scientific Polymer Products,  $M_v = 200,000 \text{ g mol}^{-1}$ ) was used after drying in a vacuum oven at  $\sim 383 \text{ K}$  to remove residual monomer. The  $T_{g,\text{bulk}}$  values measured by differential scanning calorimetry (DSC) (Mettler-Toledo, second heat, onset method,  $10 \text{ K min}^{-1}$ ) and by fluorescence agreed within experimental error: PS  $T_{g,\text{bulk}} = 375 \text{ K}$  by DSC and  $374 \text{ K}$  by fluorescence; PMMA  $T_{g,\text{bulk}} = 393 \text{ K}$  by DSC and  $391 \text{ K}$  by fluorescence; TC1-labelled PMMA  $T_{g,\text{bulk}} = 394 \text{ K}$  by DSC and  $395 \text{ K}$  by fluorescence and P2VP  $T_{g,\text{bulk}} = 373 \text{ K}$  by DSC and fluorescence. Three fluorescence dyes, pyrene (Aldrich Chemical, 99+ % purity), BPD (Molecular Probes) and 4-tricyanovinyljulolidene (TCJ; Molecular Probes), were used as received, whereas TC1 was synthesized following ref. 24. Silica nanospheres (colloidal silica in methyl ethyl ketone (MEK), Nissan Chemical Industries, reported diameter of 10–15 nm) were used as received.

### PREPARATION OF BULK FILMS AND REAL NANOCOMPOSITES

Films of neat polymers and polymer nanocomposites were prepared by spin-coating dilute solutions of polymer and dye in MEK, with or without

nanofiller, onto quartz slides. Solutions containing nanofiller were sonicated (Branson 1200 sonicator) for 40 min before spin-coating. The resulting films contained less than 0.2 wt% dye relative to polymer and were at least  $1 \mu\text{m}$  in thickness (Tencor P10 profilometer). Films were dried for at least two days in a chemical fume hood before carrying out fluorescence measurements.

Spin-coating a dilute solution is necessary to obtain the differences observed in  $T_g$  with the addition of nanoparticles to the polymer matrix. The changes in  $T_g$  reported in this study are not observed when nanocomposite films are made by solvent-casting instead of spin-coating. Solvent-casting results in much less nanoparticle dispersion in the nanocomposite film owing to aggregation that accompanies the slow drying process associated with solvent-casting.

### PREPARATION OF ULTRATHIN FILMS AND MODEL NANOCOMPOSITES

Ultrathin PMMA films were prepared by spin-coating toluene solutions onto quartz slides. The films were then dried in vacuum at  $T_g + 5 \text{ K}$  for 8 h. To prepare model nanocomposites, two films of identical thickness were spin-coated from dilute solution (PMMA in toluene or P2VP in MEK) onto quartz substrates and dried as described above. These films were brought into contact at  $T_g + 25 \text{ K}$  for 3 h and allowed to anneal, healing a portion of the interface.

### FLUORESCENCE TECHNIQUE TO DETERMINE $T_g$ AND MONITOR AGEING

Fluorescence was measured using a Spex Fluorlog-2DM1B fluorimeter and a Photon Technology International fluorimeter. Values of  $T_g$  were measured using pyrene as the dye in the PS and P2VP nanocomposites, both real and model. The BPD dye was used to measure  $T_g$  in the real PMMA nanocomposites; the TC1 label was used to characterize  $T_g$  in the PMMA model nanocomposites and ultrathin films. The  $T_g$  values were determined following a procedure outlined in refs 11,21. Physical ageing was characterized as described in refs 23,24 using TCJ as the fluorescence dye in neat polymer and polymer nanocomposite films by measuring the maximum emission intensity of TCJ (at 597–602 nm for P2VP, at 598–602 nm for P2VP-silica nanocomposites and at 590–594 nm for the model nanocomposites) as a function of ageing time after quenching from the rubbery state above  $T_g$  to 303 K.

### TRANSMISSION ELECTRON MICROSCOPY

For transmission electron microscopy (JEOL 100CX) images, dilute solutions of polymer and nanofiller were spin-coated onto grids to make films that were 50–70 nm thick. Otherwise, the preparation procedure was identical to that used for preparing the real polymer nanocomposite samples used in the fluorescence measurements.

Received 11 December 2006; accepted 21 February 2007; published 18 March 2007.

### References

- Vaia, R. A. & Giannelis, E. P. Polymer nanocomposites: Status and opportunities. *Mater. Res. Soc. Bull.* **26**, 394–401 (2001).
- Sanchez, C., Julian, B., Belleville, P. & Popall, M. Applications of hybrid organic-inorganic nanocomposites. *J. Mater. Chem.* **15**, 3559–3592 (2005).
- Keddie, J. L., Jones, R. A. L. & Cory, R. A. Size-dependent depression of the glass transition temperature in polymer films. *Europhys. Lett.* **27**, 59–64 (1994).
- van Zanten, J. H., Wallace, W. E. & Wu, W. L. Effect of strongly favorable substrate interactions on the thermal properties of ultrathin polymer films. *Phys. Rev. E* **53**, R2053–R2056 (1996).
- Forrest, J. A., Dalnoki-Veress, K., Stevens, J. R. & Dutcher, J. R. Effect of free surfaces on the glass transition temperature of thin polymer films. *Phys. Rev. Lett.* **77**, 2002–2005 (1996).
- Fryer, D. S. *et al.* Dependence of the glass transition temperature of polymer films on interfacial energy and thickness. *Macromolecules* **34**, 5627–5634 (2001).
- Grohens, Y., Hamon, L., Reiter, G., Soldera, A. & Holl, Y. Some relevant parameters affecting the glass transition of supported ultra-thin polymer films. *Eur. Phys. J. E* **8**, 217–224 (2002).
- Park, C. H. *et al.* Thickness and composition dependence of the glass transition temperature in thin random copolymer films. *Polymer* **45**, 4507–4513 (2004).
- Ellison, C. J., Kim, S. D., Hall, D. B. & Torkelson, J. M. Confinement and processing effects on glass transition temperature and physical aging in ultrathin polymer films: Novel fluorescence measurements. *Eur. Phys. J. E* **8**, 155–166 (2002).
- Ellison, C. J. & Torkelson, J. M. The distribution of glass-transition temperatures in nanoscopically confined glass formers. *Nature Mater.* **2**, 695–700 (2003).
- Ellison, C. J., Mundra, M. K. & Torkelson, J. M. Impacts of polystyrene molecular weight and modification to the repeat unit structure on the glass transition-nanoconfinement effect and the cooperativity length scale. *Macromolecules* **38**, 1767–1778 (2005).
- Mundra, M. K., Ellison, C. J., Behling, R. E. & Torkelson, J. M. Confinement, composition, and spin-coating effects on the glass transition and stress relaxation of thin films of polystyrene and styrene-containing random copolymers: sensing by intrinsic fluorescence. *Polymer* **47**, 7747–7759 (2006).
- Sharp, J. S. & Forrest, J. A. Free surfaces cause reductions in the glass transition temperature of thin polystyrene films. *Phys. Rev. Lett.* **91**, 235701 (2003).
- Roth, C. B. & Dutcher, J. R. Glass transition and chain mobility in thin polymer films. *J. Electroanal. Chem.* **584**, 13–22 (2005).

15. Alcoutlabi, M. & McKenna, G. B. Effects of confinement on material behaviour at the nanometer size scale. *J. Phys. Condens. Matter* **17**, R461–R524 (2005).
16. Ash, B. J., Schadler, L. S. & Siegel, R. W. Glass transition behavior of alumina/polymethylmethacrylate nanocomposites. *Mater. Lett.* **55**, 83–87 (2002).
17. Arrighi, V., McEwen, I. J., Qian, H. & Serrano Prieto, M. B. The glass transition and interfacial layer in styrene-butadiene rubber containing silica nanofiller. *Polymer* **44**, 6259–6266 (2003).
18. Sun, Y. Y., Zhang, Z. Q., Moon, K. S. & Wong, C. P. Glass transition and relaxation behavior of epoxy nanocomposites. *J. Polym. Sci. B* **42**, 3849–3858 (2004).
19. Berriot, J., Montes, H., Lequeux, F., Long, D. & Sotta, P. Evidence for the shift of the glass transition near the particles in silica-filled elastomers. *Macromolecules* **35**, 9756–9762 (2002).
20. Blum, F. D., Young, E. N., Smith, G. & Sitton, O. C. Thermal analysis of adsorbed poly(methyl methacrylate) on silica. *Langmuir* **22**, 4741–4744 (2006).
21. Rittigstein, P. & Torkelson, J. M. Polymer-nanoparticle interfacial interactions in polymer nanocomposites: confinement effects on glass transition temperature and suppression of physical aging. *J. Polym. Sci. B* **44**, 2935–2943 (2006).
22. Starr, F. W., Schroder, T. B. & Glotzer, S. C. Effects of a nanoscopic filler on the structure and dynamics of simulated polymer melt and the relationship to ultrathin films. *Phys. Rev. E* **64**, 021802 (2001).
23. Priestley, R. D., Broadbent, L. J. & Torkelson, J. M. Physical aging of ultrathin polymer films above and below the bulk glass transition temperature: Effects of attractive vs neutral polymer-substrate interactions measured by fluorescence. *Macromolecules* **38**, 654–657 (2005).
24. Priestley, R. D., Ellison, C. J., Broadbent, L. J. & Torkelson, J. M. Structural relaxation of polymer glasses at surfaces, interfaces, and in between. *Science* **309**, 456–459 (2005).
25. Huang, Y. & Paul, D. R. Physical aging of thin glassy polymer films monitored by optical properties. *Macromolecules* **39**, 1554–1559 (2006).
26. Kawana, S. & Jones, R. A. L. Effect of physical ageing in thin glassy polymer films. *Eur. Phys. J. E* **10**, 223–230 (2003).
27. Lu, H. B. & Nutt, S. Restricted relaxation in polymer nanocomposites near the glass transition. *Macromolecules* **36**, 4010–4016 (2003).
28. Bansal, A. *et al.* Quantitative equivalence between polymer nanocomposites and thin polymer films. *Nature Mater.* **4**, 693–698 (2005).
29. Papakonstantopoulos, G. J., Yoshimoto, K., Doxastakis, M., Nealey, P. F. & de Pablo, J. J. Local mechanical properties of polymeric nanocomposites. *Phys. Rev. E* **72**, 031801 (2005).
30. Narayanan, R. A. *et al.* Dynamics and internal stresses at the nanoscale related to unique thermomechanical behavior in polymer nanocomposites. *Phys. Rev. Lett* **97**, 075505 (2006).

#### Acknowledgements

This work was supported by the NSF-MRSEC program at Northwestern University (grants DMR-0076097 and DMR-0520513), Northwestern University and a DFI fellowship (R.D.P.). Correspondence and requests for materials should be addressed to J.M.T.

#### Competing financial interests

The authors declare no competing financial interests.

Reprints and permission information is available online at <http://npg.nature.com/reprintsandpermissions/>